Received: June 6, 2023. Revised: June 29, 2023.

INASS

International Journal of
Intelligent Engineering & Systems

http://www.inass.org/

Strategic Control in Cooperative Multi-Agent Moving Source Seeking with Obstacles Avoidance

Mochammad Sahal[1] Trihastuti Agustinah[1]* Achmad Jazidie[1] Haiping Du[2]

[1]*Electrical Engineering Department, Institut Teknologi Sepuluh Nopember, Indonesia*
[2]*School of Electrical, Computer and Telecommunications Engineering, University of Wollongong, Australia*
* Corresponding author's Email: trihastuti@ee.its.ac.id

Abstract: Agent-based moving source-seeking problem with strategic control considering obstacle avoidance is addressed in this paper. The agents communicate with one another using a communication topology to coordinate finding the object. The source or seeking target is represented by a scalar field, whereas the presence of the obstacle is represented by an artificial potential field. A moving source that moves linearly from the initial point to the end point is considered. Several obstacles, which needs to be avoided by agents, that may be stationary or moving are considered. Double integrator agents are considered, which contains richer dynamics compared to the single integrator agents. The strategic control law which is a combination of gradient consensus and distributed velocity control affected by artificial potential field are used to determine the velocity of each agent to track the moving source while avoiding the obstacles. Formation control is used to make sure that the agents stay under the desired formation for most of the time. The computer simulation is used to examine how different agents would search for a moving source under stationary and moving obstacles. In both cases, the agents can find the source with a different seeking time: 62.8s for stationary and 90s for moving obstacles. Comparing with virtual artificial potential field method, our proposed method manages to perform better in the case of shrinking agents for stationary obstacles.

Keywords: Strategic control, Gradient consensus, Obstacle avoidance, Cooperative multi-agent moving source seeking.

1. Introduction

1.1 Motivation

Source seeking problem can be defined as the problem of finding a maximum value of some potential induced by the source that describes, for example, a temperature level, the hazardous concentration of substances, etc. Some problems with cooperative source-seeking have been discussed. Prior research has studied various methods of cooperation in information-seeking tasks, and some of these ideas have been applied in real-life situations involving plants, such as unmanned aerial vehicles (UAVs) and mobile robots [1].

Source seeking algorithm is designed to drive single or multi-agents to a source represented by the scalar field signal that all the agents can measure. The scalar field is defined as a function that produces a value at every point in space. As the gradient of the scalar field signal is measured, a gradient climbing algorithm can be developed [2]. In this case, gradient estimation can be used from the distributed measurement of the scalar field of the agents.

The problem in the single-agent case is that all measurements are performed by a single agent [3] as the position changes in every instance. In this research, the estimation is conducted based on a minimum of two measurements taken from two different positions. If the sensor is sensitive enough, the agent must move further from the source to get a better signal. However, if the agent cannot detect a signal, it may remain stationary.

In the source seeking problem, the agents cooperate to measure values of the scalar field from distinct positions of agents simultaneously [4]. This allows the seeking agents to locate the right source more easily, since they have known the measured scalar field of each agent to determine the correct value of the scalar field.

In multi-agent systems, formation control is an important theme to study [5-8] because it is often used in the military and civil fields. A group of UAVs will face greater challenges when carrying out complex tasks. Apart from formation, obstacle avoidance is another thing to pay attention to. The number of UAVs makes the problem complexity higher. Unfortunaney, there is only a few references which combine formation control with source seeking, as will be discussed in the next subsection.

1.2 Related results

The issue of source-seeking has been discussed in the field of control systems, where researchers have explored several different algorithms that agents can use to locate sources of information. Moreover, there are different ways to deal with the problem of sourcing products, e.g., either focus on only one or multiple sources.

Regarding the problem of sourcing concepts for one agent, some researchers have focused on using exploratory missions to take measurements when agents change their positions regularly over time. Furthermore, for non-holonomic agents, angular velocity tuning have been proposed to find the maximum of the scalar plane of the repulsive source as mentioned earlier in [3]. Source seeking for torque-controlled unicycle is used in [1] and an approach to finding stochastic sources for non-holonomic mobile agents is presented in [9].

Over the past two decades, the topic of the formation coordinated formation control has been extensively studied with applications on multi-robot, air vehicles, underwater vehicles, and spacecraft for various fields. The main purpose of formation control is devising a strategic control that move all agents to form formation desired while guaranteeing tracking accuracy and attitude synchronization. Various advanced methods, such as the leader-follower approach [10], behaviour-based [11], and consensus-based [12], have been proposed for formation control. Among them, the leader-follower approach has been extensively studied for formation control problem. This method emphasizes the role of the leader in group, which knows the trajectory of the group globally. The leader-follower method has been discussed in formation control of mobile robots, surface vehicles, and air vehicles.

In addition, formation application in complex environments also has been studied. The examples are obstacle avoidance and communication limitations. Some of the most common methods used for obstacle avoidance are geometry-based [13], consensus-based [14], and potential-based [15]. For the potential-based method, Artificial Potential Field (APF) algorithm has been used in [16]. This method is relying on sensor data obtained by quadcopter against obstacles.

Furthermore, several algorithms for improving source-seeking performance have been developed for multi-agents. The sourcing problem can be solved by breaking it down into two parts: formation maintenance and leader-follower as shown in [17]. Formation maintenance refers to the action of ensuring that the system is organized and running smoothly. At the same time, the leader-follower part involves providing the leader with some guidance and support, so they can carry out their tasks successfully. Kalman cooperative filter is designed to estimate gradients at the center of formations in [18]. The co-evolutionary strategy for formation of missile swarm is carried out in [19].

Several studies have discussed the arrangement of formations. One example is the problem of controlling the formation of identical N agents under an unknown topology, which has been studied in [20]. In research [21], using the framework graph theory results, Popov and Werner turn the problem of formation stability into an important regulatory problem for a single agent. This way, the management of performance requirements becomes more accessible, and stability for fixed and varied topologies with communication delays is guaranteed [22].

This paper focuses on distributed velocity control for cooperative multi-agent moving source seeking under the presence of obstacles. The gradient of the scalar field helps to guide the movement of the agents, which then directs the formation towards the moving source. The agents are able to avoid both moving and obstacles in the process of reaching the source due to the presence of the artificial potential field (APF) produced by the obstacles. It is assumed that all agents are identical, and each of them has sensors to measure the intensity of the scalar field and its position relative to other agents. Each agent calculates the gradient of its measurements and those of its neighbours.

The use of APF to address obstacle avoidance problems has been considered in [23-25]. There, the authors consider n-norm for the repulsive force of APF. In this paper, the 2-norm formulation of APF is used instead. Furthermore, the attractive force part is replaced with the force from gradient consensus. Finally, unlike the stationary obstacles considered in [23-25], here a more realistic condition with moving obstacles is considered which may affect APF emitted. This becomes our strength and novelty compared to the literature reviewed.

In our previous work [26], a gradient consensus approach is considered to address the moving source problem without obstacles. In this paper, the formulation is extended to include both stationary and moving obstacles for the moving source seeking problem. Furthermore, the formulation of [26] is extended by considering a more complex systems which is a double integrator system instead of a single integrator system. The work [26] becomes the important basis of this work which consider a more complex system with obstacles. In this paper, the response of the second order systems is analyzed in tracking the moving source considering obstacle avoidance. The model of double integrator systems becomes our state of the art of this paper.

Furthermore, in this paper our method for modifying APF is compared with APF with virtual force algorithm which has been mentioned in [27]. In [27], the method of virtual force algorithm does not address the formation among agents and thus may not be suitable with our strategic control method. It will be shown that our method is able to make the agents perform better in the simulated conditions. This also becomes our state of the art of the paper.

1.3 Main contributions

In this paper, a novel strategic control law is developed which is a combination of gradient consensus and artificial potential field (APF) for the system consisting of moving source and several obstacles that need to be avoided. The main findings of this research are summarized as follows. A theoretical gradient consensus, APF-based repulsive force, and distributed velocity control are proposed for cooperative multi-agent moving source seeking under the presence of obstacles. By incorporating these elements, the APF-based repulsive force algorithm is modified in order to improve the performance of the agents especially in a shrinking agent condition. This paper proposes a new unique strategy in the form of novel APF-based repulsive force algorithm to address source seeking and obstacle avoidance problems. To our best knowledge, our paper is the first to address formation control problem combined with gradient consensus and Modified APF.

1.4 Outline

The organization of the paper is specified as follows. In section 2, the problem formulations and multi-agent model are outlined. Then, the methods consisting of gradient consensus, artificial potential field, and strategic control in sections 3, 4, and 5, respectively. The main results in the form of simulations are shown in section 6. The paper is concluded in section 7.

1.5 Notation

The notations in this paper are described in Table 1 as follows. The interaction of agents is modeled by a connected and undirected graph $G = (V, E)$. Edge $(i,j) = (j,i) \in E$ indicates that agent i sends information to agent j (and vice versa). The adjacency matrix representing communication among agents of graph G is denoted by symmetric matrix $A = [a_{ij}] \in \mathbb{R}^{N\times N}$, where $a_{ij} = 1$ if $(i,j) \in E$ and $a_{ij} = 0$ otherwise.

2. Scalar field of the source

In this section, the scalar field of the source is explained. Generally, the agents are supposed to reach the moving source which generates the scalar field.

Here a scalar field $\psi = \psi(r)$ is considered which is a mapping of $\psi\colon \mathbb{R}^P \to \mathbb{R}^+$, where $p =$

Table 1. Some notations used in this paper

Notation	Description
$G = (V, E)$	Graph
$V = \{1,2,\dots,N\}$	Vertices
$E \subseteq V\times V$	Edges
$L \in \mathbb{R}^{N\times N}$	Laplacian matrix
$\Delta \in \mathbb{R}^{N\times N}$	Degree matrix
$A \in \mathbb{R}^{N\times N}$	Adjacency matrix
$N_i = \{i \in V: a_{ij} \neq 0\}$	Neighbors of agent i
$\mathbf{1} = [1\ 1 \dots 1]^\top \in \mathbb{R}^N$	Column vector with 1 as its element.
$\otimes$	Kronecker product
r=$[x\ y]^T$	Position
ψ	Scalar field
$I_N \in \mathbb{R}^{N\times N}$	Identity matrix
α	Expansion coefficient
$\hat{g}$	Gradient estimation
$\dot{g}$	Gradient consensus
β	Consensus parameter
U_{rep}	Repulsive field
F_{rep}	Repulsive Force
k_{rep}	Repulsive coefficient
k_{vir}	Virtual force gain
r	Position
v	Velocity
u	Accelerator, control signal
k_f	Formation coefficient
k_v	Velocity coefficient
k_r	Repulsive control coefficient
γ	Velocity agent coefficient

Received: June 6, 2023. Revised: June 29, 2023.

$1, 2,$ or 3 denoting the dimension and $r \in \mathbb{R}^p$ defining the position coordinate of the agent in space. In this paper the two-dimension case, i.e., $p = 2, r = [x\ y]^\top \in \mathbb{R}^2$ is assumed. The source is located at the maximum value of ψ, which the agents attempt to reach. Specifically, the agents attempt to find the value of $r(t)$ that maximizes the scalar field ψ. This can be formulated by the following optimization equation

$$r^* = arg\ max\ \psi(r).$$

Initially, the static source scalar function is used first at $t = 0$, followed by the moving source scalar function. The static source scalar function containing one peak and combination of two different contours as shown in Fig. 1 is formulated as follows:

$$\psi_s(x, y) = A_1 e^{-\frac{(x-x_1)^2}{\sigma_{x_1}^2} - \frac{(y-y_1)^2}{\sigma_{y_1}^2}} + A_2 e^{-\frac{(x-x_2)^2}{\sigma_{x_2}^2} - \frac{(y-y_2)^2}{\sigma_{y_2}^2}} \quad (1)$$

At $t > 0$, the peak (also called maximum) of the scalar function at $(x, y) = (x_1, y_1) = (x_2, y_2)$ moves with a certain speed according to the movement of the source: linear and sinusoidal movement. Throughout this paper, it is assumed that the moving scalar field of source $\psi(r)$ has only a single maximum and no local maximum.

On the linear movement part, the source moves with constant scalar speed v_x, v_y on the x-axis and y-axis as

$$x_x(t) = v_x t[1\ 1]^\top \quad (2)$$

$$x_y(t) = v_y t[1\ 1]^\top \quad (3)$$

where $x_x = [x_1\ x_2]^\top$ and $x_y = [y_1\ y_2]^\top$ denote the position of the peak on the x-axis and y-axis, respectively.

It is also considered that the scalar field can scale in the form of expansion or contraction. Specifically, using the scaling function formula, the scaling movement of the scalar function with scaling period t_s is specified as

$$\boldsymbol{\sigma}(t + t_s) = \alpha(\boldsymbol{\sigma}(t)) \quad (4)$$

where $\boldsymbol{\sigma} = \left[\sigma_{x_1}\ \sigma_{y_1}\ \sigma_{x_2}\ \sigma_{y_2}\right]^\top$. The movement of $\boldsymbol{\sigma}$ in Eq. (4) can be categorized as expansion or contraction if $\alpha > 1$ or $\alpha < 1$, respectively. Here, both expansion and contraction cases are considered in the same experiment, i.e., the value of α may switch over time.

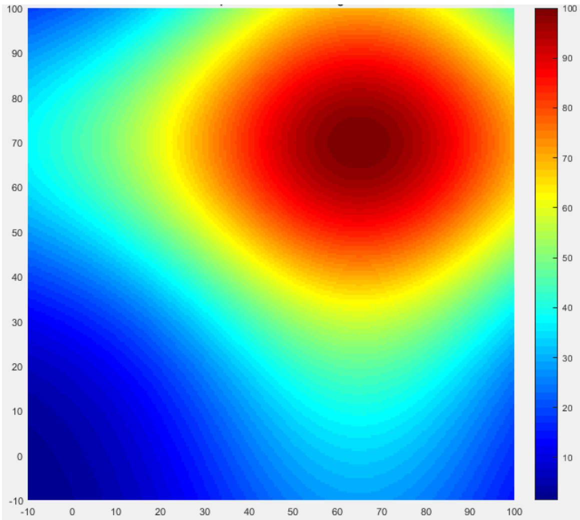

Figure. 1 Example of scalar field $\boldsymbol{\psi}$

3. Gradient estimation and gradient consensus

This section discusses the gradient estimation of each agent and the gradient consensus of the formation of cooperative multi-agent in source seeking.

3.1 Gradient estimation

In the multi-agent-based gradient estimation, each agent approximates its own gradient, and the connected agents receive the estimations from their neighbours to compute the global gradient. The proposed method to compute the gradient estimation is based on the least squares [28, 29].

Each agent i measures the intensity of the scalar field ψ from its position. This is denoted by $\psi_i = \psi(r_i)$, where $i = 1, 2, 3, \ldots N$. Given the position of agent j, r_j, that is close to agent i, r_i, the estimation can be calculated by using the first-order Taylor series. The estimation of ψ_j at r_i is given by:

$$\psi(r_j) \approx \psi(r_i) + (r_j - r_i)^\top \hat{\boldsymbol{g}}(r_i) \quad (5)$$

where $\hat{\boldsymbol{g}}(r_i)$ is the estimated gradient calculated by agent i. For $p = 2$, the estimated gradient becomes $\hat{\boldsymbol{g}}(r_i) = \left[\hat{\boldsymbol{g}}_x(r_i)\hat{\boldsymbol{g}}_y(r_i)\right]^\top$. If agent i has $|N_i|$ neighbours, then Eq. (5) becomes

$$\begin{bmatrix} \psi(r_1) - \psi(r_i) \\ \psi(r_2) - \psi(r_i) \\ \vdots \\ \psi(r_{|N_i|}) - \psi(r_i) \end{bmatrix} = \begin{bmatrix} (r_1 - r_i)^\top \\ (r_2 - r_i)^\top \\ \vdots \\ (r_{|N_i|} - r_i)^\top \end{bmatrix} \hat{\boldsymbol{g}}(r_i) \quad (6)$$

$$b_i = A_i \hat{g}_i \tag{7}$$

where $b_i \in \mathbb{R}^{|N_i| \times 1}, A_i \in \mathbb{R}^{||N_i|| \times p}$, and $\boldsymbol{\hat{g}_i} \in \mathbb{R}^{p \times 1}$. This problem can be solved by using the least-squares method

$$\hat{g}_i = \left(A_i^{\top} A_i\right)^{-1} A_i^{\top} b_i \tag{8}$$

which can be written in integrated form as

$$\hat{g} = \hat{g}_i \otimes \; I_N \tag{9}$$

where agent $i = 1, \ldots, 7$.

3.2 Gradient of the consensus filter

The consensus algorithm proposed by Olfati-Saber and Shamma in [30] is the average consensus filter for spatially distributed sensor networks. In this algorithm, each sensor receives inputs from its neighbours, estimates them, and then averages them. The average consensus was applied to gradient consensus as follows

$$\dot{g}_i = \beta \sum_{j \epsilon N_i} a_{ij} e_{g_{ij}}(t) + \beta(1 + d_i)\big(\hat{g}_i(t) - g_i(t)\big), \tag{10}$$

where

$$e_{g_{ij}}(t) = \big(\hat{g}_i(t) - g_i(t)\big) - \left(\hat{g}_j(t) - g_j(t)\right)$$

and $\beta \geq 1$ is a control parameter for tracking the performance of the gradient as the agent moves. By using the definition of the Laplacian graph, the following equation is obtained:

$$\begin{aligned} \dot{g} = &-\beta\big(I_N \otimes I_p + \Delta \otimes I_p + L \otimes I_p\big) g \\ &+\beta\big(I_N \otimes I_p + \Delta \otimes I_p + L \otimes I_p\big)\hat{g} \end{aligned} \tag{11}$$

where $I_N \in \mathbb{R}^{N \times N}$ and $I_p \in \mathbb{R}^{p \times p}$ are identity matrices. Thus Eq. (11) can be rewritten as:

$$\dot{g} = \beta\big(A_g g + B_g \hat{g}\big) \tag{12}$$

where $A_g = -B_g$ and $B_g = I_N \otimes I_p + \Delta \otimes I_p + L \otimes I_p$, $B \in \mathbb{R}^{Np \times Np}$.

4. Artificial potential field of the obstacles

In this section, the obstacles and the associated Artificial Potential Field are explained. Generally, the agents are supposed to avoid the obstacles along the way of trying to reach the source.

The artificial potential field (APF) method used is the modified one, namely optimal APF. The algorithm is developed through a scenario where an agent moves in a two-dimensional space with position $X = (x, y)^T$.

APF has been used widely on the path planning problem considering obstacles. In what follows, the proposed APF called by the modified APF (MAPF) used in this paper will be compared to APF with virtual force algorithm (VAPF) in proposed in [27]. The authors in [27] consider APF with virtual force algorithm with repulsion force as

$$F_{rep}(X) = -\nabla\big(U_{rep}\big) = \begin{cases} F_{rep1}(X) + F_{vir}(X), & for\ \rho(X) \leq \rho_0 \\ 0, & for\ \rho(X) > \rho_0 \end{cases} \tag{13}$$

where,

$$F_{rep1}(X) = k_r \left(1 - \frac{\rho(X)}{\rho_0}\right) \frac{1}{\rho^2(X)} \tag{14}$$

$$F_{vir}(X) = -k_{vir} \frac{1}{\rho(X)} \tag{15}$$

and k_{vir} is the virtual force gain.

In this paper, the repulsive field U_{rep} from obstacles affects the agent movement

$$U_{rep}(X) = \begin{cases} \frac{1}{2} k_{rep} \left(\frac{1}{\rho(X)} - \frac{1}{\rho_0}\right)^2 \rho_t(X), \\ \qquad for\ \rho(X) \leq \rho_0 \\ 0, \\ \qquad for\ \rho(X) > \rho_0 \end{cases} \tag{16}$$

The repulsive force is then derived from the control signal.

$$F_{rep}(X) = -\nabla\big(U_{rep}\big) = \begin{cases} F_{rep1}(X), & for\ \rho(X) \leq \rho_0 \\ 0, & for\ \rho(X) > \rho_0 \end{cases} \tag{17}$$

where

$$F_{rep1}(X) = k_{rep} \left(\frac{1}{\rho(X)} - \frac{1}{\rho_0}\right) \frac{\rho_t(X)}{\rho(X)^2} \frac{\partial \rho(X)}{\partial(X)} \tag{18}$$

where F_{rep} is the repulsive force from obstacle. The forces are added to the agents' current position and become reference position for the flight controller. As for supporting the process of maintaining the formation, the value will be varied if it meets certain criteria, such that on some occasion the leader will slow down, and the follower will accelerate at the same time.

5. Strategic control for moving source seeking

Generally, the agents are supposed to avoid the obstacles along the way of trying to reach the source.

A double integrator agent model is considered

$$\dot{r}_i(t) = v_i(t) \tag{19}$$

$$\dot{v}_i(t) = u_i(t) \tag{20}$$

where

$$u_i(t) = k_F \sum_{j \in \mathcal{N}_i} a_{ij} \left[\left(r_{Fi}(t) - r_{Fj}(t) \right) - \left(r_i(t) - r_j(t) \right) \right] + k_v \left(\hat{g}_i(t) - \gamma v_i(t) \right) + k_r F_{rep} \tag{21}$$

where the coefficients $k_F, k_v, \ \gamma, k_r$ are nonnegative. The coefficients k_F and k_v denote the weight of movement based on formation control and velocity tracking, respectively. The integrated cooperative multi-agent model from Eqs. (19)-(21) became

$$\dot{\boldsymbol{x}} = \boldsymbol{A_m x} + \boldsymbol{B_m u} \tag{22}$$

where

$$\boldsymbol{x} = [x_1 \dots x_n]^\top, \text{where } x_i = \begin{bmatrix} r \\ v \end{bmatrix} \tag{23}$$

$$\boldsymbol{u} = [u_1 \dots u_n]^\top, \text{where } u_i = \begin{bmatrix} r_F \\ \hat{g}(r) \end{bmatrix} \tag{24}$$

Since a double integrator agent model is considered,

$$\boldsymbol{A_m} = A_{m_i} \otimes I_N \tag{25}$$

$$\boldsymbol{B_m} = B_{m_i} \otimes I_N \tag{26}$$

where

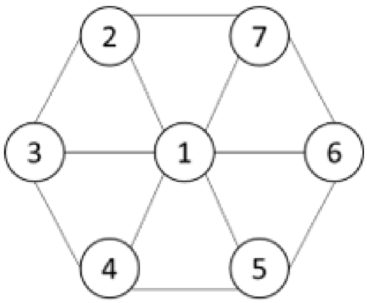

Figure. 2 Formation used in the simulations

$$A_{m_i} = \begin{bmatrix} 0 & 1 & 0 & 0 & 0 & 0 \\ 0 & 0 & 0 & 0 & 0 & 0 \\ 0 & 0 & 0 & 1 & 0 & 0 \\ 0 & 0 & 0 & 0 & 0 & 0 \\ 0 & 0 & 0 & 0 & 0 & 1 \\ 0 & 0 & 0 & 0 & 0 & 0 \end{bmatrix} \tag{27}$$

$$B_{m_i} = \begin{bmatrix} 0 & 0 & 0 \\ 1 & 0 & 0 \\ 0 & 0 & 0 \\ 0 & 1 & 0 \\ 0 & 0 & 0 \\ 0 & 0 & 1 \end{bmatrix} \tag{28}$$

and I_N being identity matrix with dimension $N \times N$. Algorithm 1 specifies the strategic control of cooperative multi-agents moving source seeking with obstacles avoidance.

6. Simulation results

In this section, some numerical examples are provided for moving source seeking under obstacle avoidance. Linearly moving source with stationary and moving obstacle is considered, with and without agent shrinking. The parameters used for control signal $u_i(t)$ are $k_F = 0.5$, $k_v = 6$, $k_{rep} = 0.01$, $k_r = 1, \gamma = 0.5$, and $\beta = 1$.

In the figures shown throughout this section, the graph as shown in Fig. 2 is considered. Agent #1, which is positioned in the center of the graph, is the important agents and will be used to indicate the graph and other agents' position throughout the field.

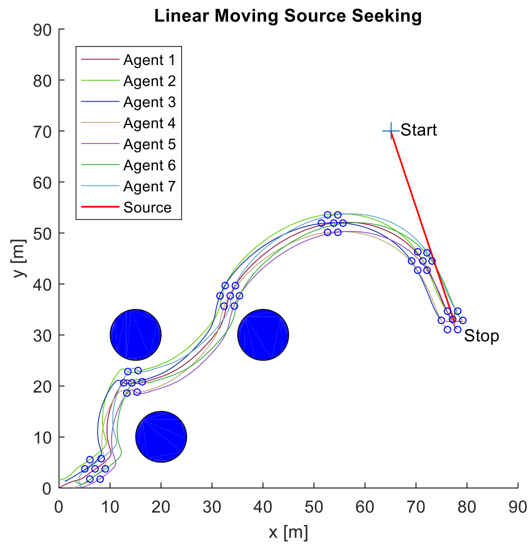

Figure. 3 Obstacle avoidance trajectories for stationary obstacles with modified APF (MAPF) See animated for Figs. 3, 5, 7, 9, 11, and 13: http://bit.ly/MovingSourceSeekingWithObstaclesAvoidance

Algorithm 1. Strategic control of cooperative multi-agents moving source seeking with obstacles avoidance

INPUT:
time sampling T_s, end simulation E_s, initial position agents r, position formation agents r_f, parameters of cooperative multi-agent $k_F, k_v, k_r, \beta, \gamma$, parameters of moving source $A_1, x_1, y_1, \sigma_{x1}, \sigma_{y1}, A_2, x_2, y_2, \sigma_{x2}, \sigma_{y2}, v_x, v_y, A, \omega,$
,
parameters of artificial potential field K_{rep}, ρ_0, K_{att}, Matrices of consensus gradient system and model system $\boldsymbol{A}_g, \boldsymbol{B}_g, \boldsymbol{A}_m, \boldsymbol{B}_m$, Obstacles $\boldsymbol{O}_s$

OUTPUT: trajectories of all agents
for t = 0 to E_s step T_s
$\psi_s(x, y) \leftarrow x, y$ %moving source by Eq. (1)
Strategic Control:
$\widehat{\boldsymbol{g}} \leftarrow g_i$ %gradient estimation by Eq. (9)
$\dot{\boldsymbol{g}} \leftarrow \widehat{\boldsymbol{g}}$ %gradient consensus by Eq. (12)
if $\rho(X) \le \rho_0$
$\boldsymbol{F}_{rep} \leftarrow \rho(X), \rho_t(X)$ %repulsive forces Eq. (17)
if $d_o(X) \le d_0$
$r_f \leftarrow \varsigma$ %shrinking formation
$\boldsymbol{u} \leftarrow r, r_f, \widehat{\boldsymbol{g}}, \boldsymbol{F}_{rep}$ %control signal by Eq. (24)
$\boldsymbol{x} \leftarrow \boldsymbol{x}, \boldsymbol{u}$ %model state by Eq. (22)
$\boldsymbol{r} \leftarrow \boldsymbol{x}$ %agents position by Eq. (23)
$\boldsymbol{d}_{a1\_o} \leftarrow \boldsymbol{r}, \boldsymbol{O}_s$ %distance of agent #1 and three obstacles
end
return $\boldsymbol{r}, \boldsymbol{d}_{a1\_o}$

Fig. 3 shows obstacle avoidance trajectories under three obstacles and a source moving linearly whereas Fig. 4 illustrates the distance between the moving agent 1 and the three obstacles. From those figures, it can be seen that agents are able to catch the source while avoiding the three stationary obstacles.

From Figs. 5 and 6, it can be seen that the agents can both maintain formation and avoiding the obstacles with a tight space between obstacles. This can be achieved by performing a shrinking maneuver of the agents. As seen in Fig. 5, at around 20s the position of agents become more compact due to tighter space between obstacles.

Furthermore, Fig. 7 shows obstacle avoidance trajectories under two stationary obstacles and one moving obstacle that moves upward with the distance shown in Fig. 8. From those figures, it can be seen that agents are able to catch the source while also avoiding a moving obstacle.

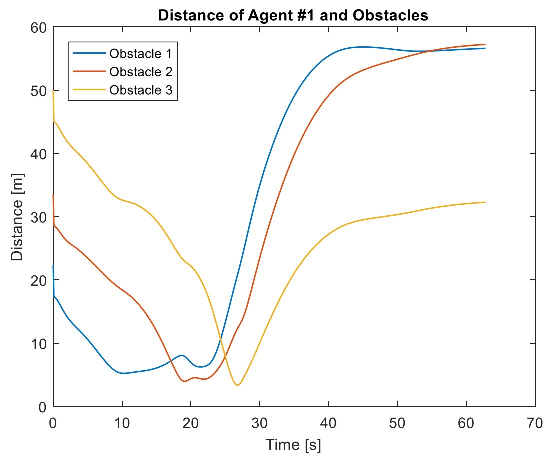

Figure. 4 Distance between the obstacles and Agent #1 over time with modified APF (MAPF)

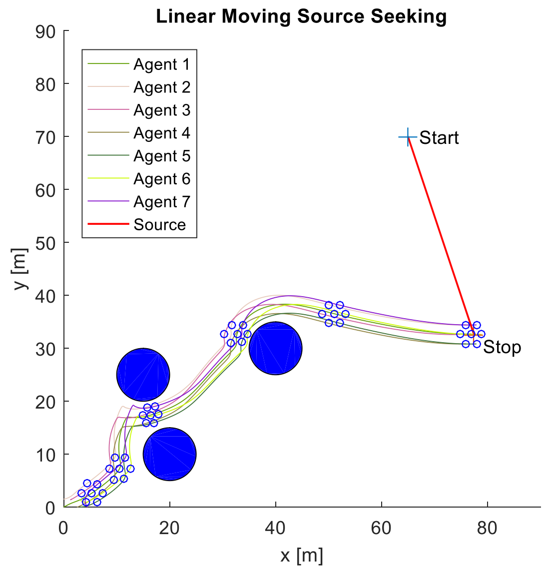

Figure. 5 Obstacle avoidance trajectories for stationary obstacles with shrinking formation and MAPF

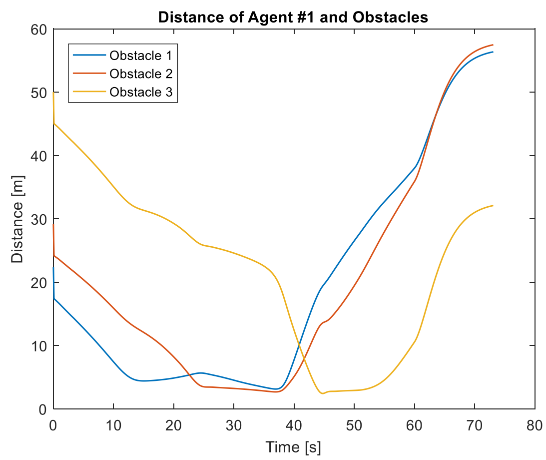

Figure. 6 Distance between the obstacles and Agent #1 over time for shrinking formation and MAPF

Received: June 6, 2023. Revised: June 29, 2023.

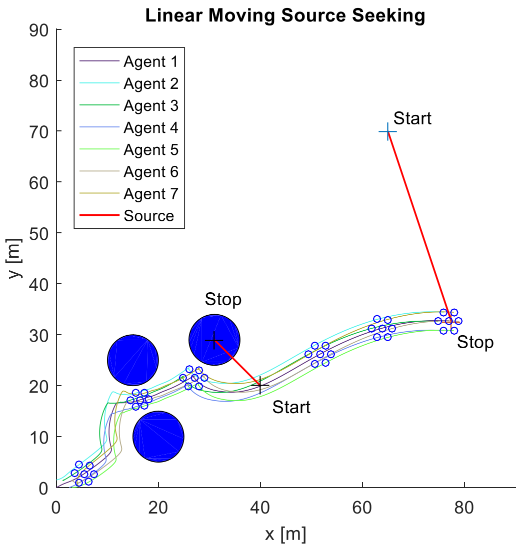

Figure. 7 Obstacle avoidance trajectories for moving obstacles and MAPF

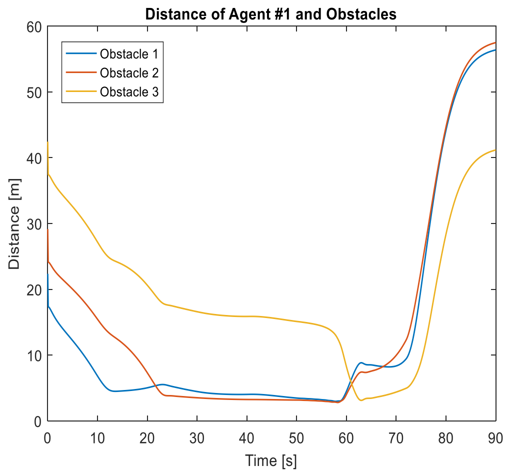

Figure. 8 Distance between the obstacles and Agent #1 over time for moving obstacles and MAPF

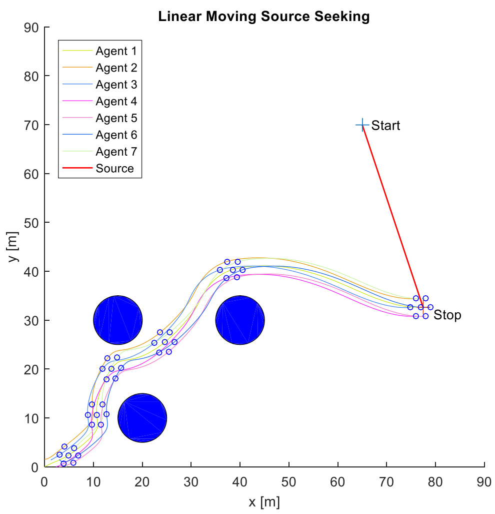

Figure. 9 Obstacle avoidance trajectories for stationary obstacles with virtual APF (VAPF)

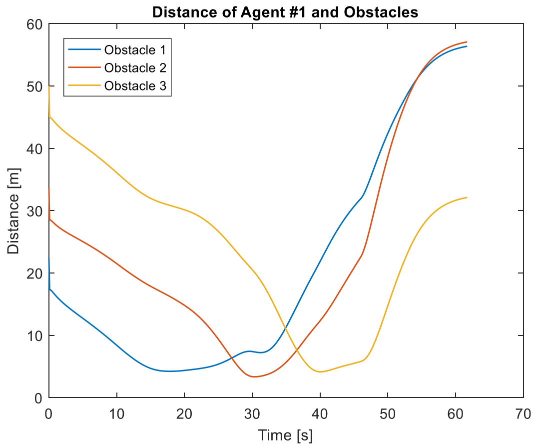

Figure. 10 Distance between the obstacles and Agent #1 over time with virtual APF (VAPF)

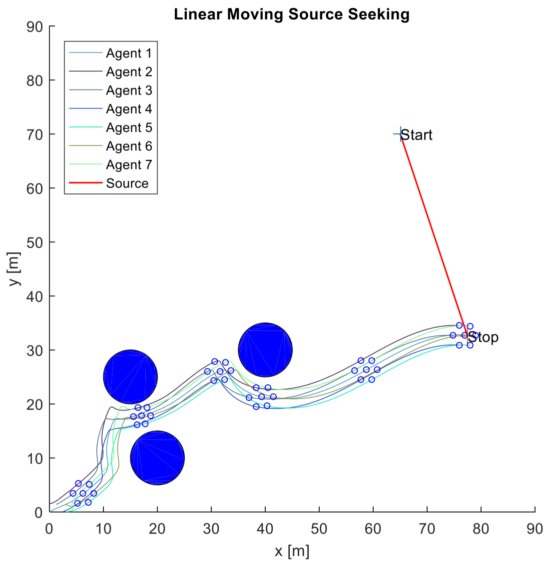

Figure. 11 Obstacle avoidance trajectories for stationary obstacles with shrinking agents and virtual APF

The result is further compared with the virtual APF defined in Eq. (13). Specifically, the figures associated with stationary obstacles, stationary obstacles with shrinking movements, and moving obstacles with shrinking movements are shown. From Figs. 9-14, it can be seen that the agents can reach the source in all cases.

The minimum distance between Agent #1 and each of the three obstacles as well as the time needed to reach the moving source for both MAPF and VAPF is illustrated in Table 2. It can be seen that in both methods the agents reach the source fastest when the obstacles are all stationary. On the other hand, the agents reach the source slowest in both methods when the obstacles move, since they have to maneuver to avoid the more agile obstacles.

Table 2 shows the comparison between our proposed method (MAPF) versus VAPF. The variable

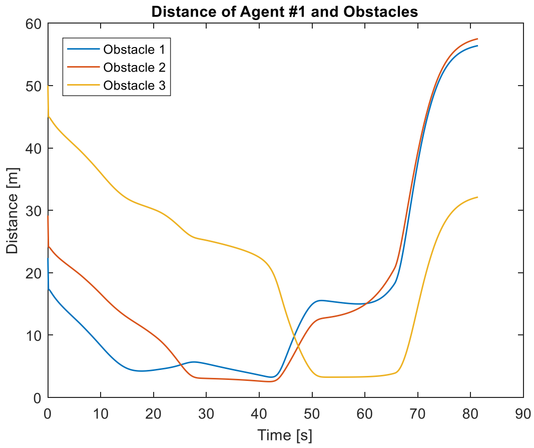

Figure. 12 Distance between the obstacles and Agent #1 over time with shrinking agents and virtual APF

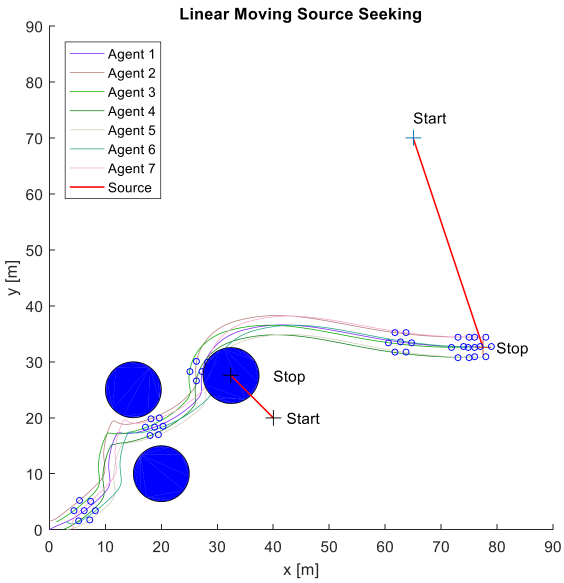

Figure. 13 Obstacle avoidance trajectories for stationary obstacles considering moving obstacle with virtual APF

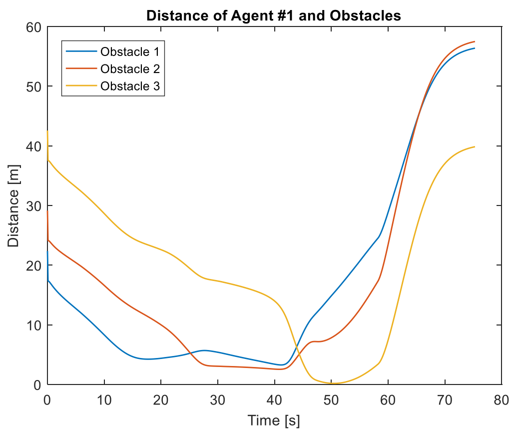

Figure. 14 Distance between the obstacles and Agent #1 over time considering moving obstacle with virtual APF

Table 2. Minimum distance between Agent #1 and the three obstacles with modified and virtual APF

No	Experiment	min dist1 (m)	min dist2 (m)	min dist3 (m)	Time (sec)
1	Static: MAPF	5.25	3.98	3.37	62.8
2	Static: VAPF	4.22	3.34	4.14	61.7
3	Shrink: MAPF	3.13	2.68	2.43	73.1
4	Shrink: VAPF	3.26	2.54	3.26	81.4
5	Shrink+Move: MAPF	2.97	2.80	3.12	90
6	Shrink+Move: VAPF	3.27	2.54	0.17	75.3

'min dist' is the minimum distance with the edge of the obstacles. Three 'min dist' are considered because there are three obstacles. Three experiments are conducted: static obstacles, static obstacles with shrinking agents, and moving obstacles with shrinking agents. It is shown that in all experiments, the minimum distance is more than the allowable distance.

From Table 2, it is observed that in an environment with modified APF, the agents may reach the source faster by 8.3s or about 10.2%. However, for the situation where agents need to shrink to avoid obstacles, it is shown that our algorithm may perform better compared to VAPF.

7. Conclusion

In this paper, a strategic control is considered, which is a combination of gradient consensus and artificial-potential-function-based velocity control of a multi-agent system that pursue a moving source while avoiding obstacles. Gradient-based approach is used to derive the velocity of the agents, which are tasked to trace the position of a moving source while avoiding the obstacles that emits certain repulsive force under the framework of artificial potential field (APF). Under this gradient-based and APF-based strategic velocity control, it is shown that the agents are able to reach the moving source while avoiding both moving and stationary obstacles. Several numerical examples are provided to give a performance comparison between the agents under several conditions. It is shown that our proposed method combining gradient consensus with APF may perform better compared to virtual APF in the scenario where agents need to shrink due to small gaps between obstacles with time needed to reach the source 73.1s versus 81.4s of VAPF method.

Conflicts of interest

The authors declare no conflict of interest.

Received: June 6, 2023. Revised: June 29, 2023.

Author contributions

Conceptualization, M.S.; methodology, M.S.; software, M.S.; validation, M.S.; formal analysis, M.S.; investigation, M.S.; resources, M.S.; data curation, M.S.; writing original draft preparation, M.S.; writing review and editing, M.S., T.A., and A.J..; visualization, M.S.; supervision, T.A., A.J., and H.D.

Acknowledgments

This work was supported by the Laboratory of Systems and Cybernetics and Laboratory of Control and Automation, and the PT Infoglobal Teknologi Semesta. The authors would like to thank the Laboratory of Systems and Cybernetics and Laboratory of Control and Automation, Department of Electrical Engineering, Institut Teknologi Sepuluh Nopember for allowing authors to use the research facilities, and the PT Infoglobal Teknologi Semesta for funding.

References

[1] R. Suttner and M. Krstic, "Source Seeking With a Torque-Controlled Unicycle", *IEEE Control Syst Lett*, Vol. 7, pp. 79–84, 2023, doi: 10.1109/LCSYS.2022.3186837.

[2] B. P. Huynh, C. W. Wu, and Y. L. Kuo, "Force/Position Hybrid Control for a Hexa Robot Using Gradient Descent Iterative Learning Control Algorithm", *IEEE Access*, Vol. 7, pp. 72329–72342, 2019, doi: 10.1109/ACCESS.2019.2920020.

[3] V. Todorovski and M. Krstic, "Prescribed-Time Seeking of a Repulsive Source by Angular Velocity Tuning", In: *Proc. of 2022 American Control Conference (ACC)*, pp. 8–13, 2022, doi: 10.23919/ACC53348.2022.9867214.

[4] B. A. Angelico, L. F. O. Chamon, S. Paternain, A. Ribeiro, and G. J. Pappas, "Source Seeking in Unknown Environments with Convex Obstacles", In: *Proc. of 2021 American Control Conference (ACC)*, pp. 5055–5061, 2021, doi: 10.23919/ACC50511.2021.9483164.

[5] Z. Cai, L. Wang, J. Zhao, K. Wu, and Y. Wang, "Virtual target guidance-based distributed model predictive control for formation control of multiple UAVs", *Chinese Journal of Aeronautics*, Vol. 33, No. 3, pp. 1037–1056, 2020, doi: 10.1016/j.cja.2019.07.016.

[6] L. Cao, D. Yao, H. Li, W. Meng, and R. Lu, "Fuzzy-based dynamic event triggering formation control for nonstrict-feedback nonlinear MASs", *Fuzzy Sets Syst*, Vol. 452, pp. 1–22, 2023, doi: 10.1016/j.fss.2022.03.005.

[7] S. Li, X. Wang, S. Wang, and Y. Zhang, "Distributed Bearing-Only Formation Control for UAV-UWSV Heterogeneous System", *Drones*, Vol. 7, No. 2, p. 124, 2023, doi: 10.3390/drones7020124.

[8] B. S. Chen, Y. C. Liu, M. Y. Lee, and C. L. Hwang, "Decentralized H PID Team Formation Tracking Control of Large-Scale Quadrotor UAVs Under External Disturbance and Vortex Coupling <sub/>", *IEEE Access*, Vol. 10, pp. 108169–108184, 2022, doi: 10.1109/ACCESS.2022.3211663.

[9] S. I. Azuma, M. S. Sakar, and G. J. Pappas, "Stochastic source seeking by mobile robots", *IEEE Trans Automat Contr*, Vol. 57, No. 9, pp. 2308–2321, 2012, doi: 10.1109/TAC.2012.2186927.

[10] J. Ghommam and M. Saad, "Adaptive Leader–Follower Formation Control of Underactuated Surface Vessels Under Asymmetric Range and Bearing Constraints", *IEEE Trans Veh Technol*, Vol. 67, No. 2, pp. 852–865, 2018, doi: 10.1109/TVT.2017.2760367.

[11] J. Wen, J. Yang, Y. Li, J. He, Z. Li, and H. Song, "Behavior-Based Formation Control Digital Twin for Multi-AUG in Edge Computing", *IEEE Trans Netw Sci Eng*, pp. 1–11, 2022, doi: 10.1109/TNSE.2022.3198818.

[12] H. Rezaee and F. Abdollahi, "Pursuit Formation of Double-Integrator Dynamics Using Consensus Control Approach", *IEEE Transactions on Industrial Electronics*, Vol. 62, No. 7, pp. 4249–4256, 2015, doi: 10.1109/TIE.2014.2384479.

[13] X. Shi, Q. Ye, X. Chen, C. Chen, Z. Chen, and T. K. Kim, "Geometry-based Distance Decomposition for Monocular 3D Object Detection", In: *Proc. of 2021 IEEE/CVF International Conference on Computer Vision (ICCV)*, pp. 15152–15161, 2021, doi: 10.1109/ICCV48922.2021.01489.

[14] J. Zhang, J. Yan, P. Zhang, and X. Kong, "Collision Avoidance in Fixed-Wing UAV Formation Flight Based on a Consensus Control Algorithm", *IEEE Access*, Vol. 6, pp. 43672–43682, 2018, doi: 10.1109/ACCESS.2018.2864169.

[15] J. Zhang, J. Yan, and P. Zhang, "Fixed-wing UAV formation control design with collision avoidance based on an improved artificial potential field", *IEEE Access*, Vol. 6, pp. 78342–78351, 2018, doi: 10.1109/ACCESS.2018.2885003.

[16] Z. Pan, C. Zhang, Y. Xia, H. Xiong, and X.

Shao, "An Improved Artificial Potential Field Method for Path Planning and Formation Control of the Multi-UAV Systems", *IEEE Transactions on Circuits and Systems II: Express Briefs*, Vol. 69, No. 3, pp. 1129–1133, 2022, doi: 10.1109/TCSII.2021.3112787.

[17] P. Ogren, E. Fiorelli, and N. E. Leonard, "Cooperative Control of Mobile Sensor Networks: Adaptive Gradient Climbing in a Distributed Environment", *IEEE Trans Automat Contr*, Vol. 49, No. 8, pp. 1292–1302, 2004, doi: 10.1109/TAC.2004.832203.

[18] F. Zhang and N. E. Leonard, "Cooperative filters and control for cooperative exploration", *IEEE Trans Automat Contr*, Vol. 55, No. 3, 2010, doi: 10.1109/TAC.2009.2039240.

[19] J. Chen, X. Lan, Y. Zhou, and J. Liang, "Formation Control with Connectivity Assurance for Missile Swarms by a Natural Co-Evolutionary Strategy", *Mathematics*, Vol. 10, No. 22, p. 4244, 2022, doi: 10.3390/math10224244.

[20] J. A. Fax and R. M. Murray, "Information flow and cooperative control of vehicle formations", *IEEE Trans Automat Contr*, Vol. 49, No. 9, 2004, doi: 10.1109/TAC.2004.834433.

[21] A. P. Popov and H. Werner, "A robust control approach to formation control", In: *Proc. of 2009 European Control Conference, ECC 2009*, 2014, doi: 10.23919/ecc.2009.7075097.

[22] M. Sahal, T. Agustinah, and A. Jazidie, "Switching Formation and Topology in Cooperative Multi-Agent Source Seeking Using Gradient Estimation", In: *Proc of 2019 International Conference of Artificial Intelligence and Information Technology, ICAIIT 2019*, 2019, doi: 10.1109/ICAIIT.2019.8834525.

[23] P. Wang, S. Gao, L. Li, B. Sun, and S. Cheng, "Obstacle Avoidance Path Planning Design for Autonomous Driving Vehicles Based on an Improved Artificial Potential Field Algorithm", *Energies (Basel)*, Vol. 12, No. 12, p. 2342, 2019, doi: 10.3390/en12122342.

[24] A. M. Arif, W. Rahmaniar, M. A. M. Vera, A. A. Nuryono, R. Majdoubi, and A. Cakan, "Artificial Potential Field Algorithm for Obstacle Avoidance in UAV Quadrotor for Dynamic Environment", In: *Proc. of 2021 IEEE International Conference on Communication, Networks and Satellite (COMNETSAT), IEEE*, pp. 184–189, 2021, doi: 10.1109/COMNETSAT53002.2021.9530803.

[25] S. M. H. Rostami, A. K. Sangaiah, J. Wang, and X. Liu, "Obstacle avoidance of mobile robots using modified artificial potential field algorithm", *EURASIP J Wirel Commun Netw*, Vol. 2019, No. 1, p. 70, 2019, doi: 10.1186/s13638-019-1396-2.

[26] M. Sahal, T. Agustinah, A. Jazidie, and H. Du, "Distributed Velocity Control in Cooperative Multi-Agent Moving Source Seeking", *Przegląd Elektrotechniczny*, 2023.

[27] I. Iswanto, A. Ma'arif, O. Wahyunggoro, and A. Imam, "Artificial Potential Field Algorithm Implementation for Quadrotor Path Planning", *International Journal of Advanced Computer Science and Applications*, Vol. 10, No. 8, 2019, doi: 10.14569/IJACSA.2019.0100876.

[28] E. Rosero and H. Werner, "Cooperative source seeking via gradient estimation and formation control (Part 1)", In: *Proc. of 2014 UKACC International Conference on Control, CONTROL 2014*, 2014, doi: 10.1109/CONTROL.2014.6915212.

[29] M. Sahal, "Comparison of Gradient Estimation in Cooperative Multi-Agent Source Seeking", *Journal on Advanced Research in Electrical Engineering*, Vol. 1, No. 2, 2017, doi: 10.12962/j25796216.v1.i2.21.

[30] R. O. Saber and J. S. Shamma, "Consensus filters for sensor networks and distributed sensor fusion", In: *Proc of the 44th IEEE Conference on Decision and Control, and the European Control Conference, CDC-ECC '05*, 2005, doi: 10.1109/CDC.2005.1583238.